World Conference on Timber Engineering Oslo 2023

NUMERICAL MODELLING OF A CROSS-LAMINATED TIMBER-TO-CONRETE DOWEL-TYPE CONNECTION USING THE BEAM-ON-FOUNDATION MODEL

Joan W. Gikonyo[1], Eva Binder[2], Michael Schweigler[3], Thomas K. Bader[4]

ABSTRACT: The aim of the research presented herein is to investigate the mechanical behaviour of cross-laminated timber (CLT)-to-concrete dowel-type connections. For reliable timber-concrete-composite structures, mechanical connections between the two construction materials are of great importance. This paper investigates the nonlinear load-displacement behaviour, giving access to the stiffness and strength, as well as ductile connection failure modes, of a CLT-to-concrete composite connection using a Beam-on-Foundation (BoF) model. The latter is a numerical model that utilizes non-linear springs for the interaction between the fastener and the surrounding CLT and concrete materials. The influence of: (i) fastener diameter, (ii) initial slip, (iii) concrete embedment properties, and (iv) axial fastener resistance due to friction, on the connection shear capacity and slip modulus, was investigated in a parameter study. The nonlinear load-displacement response, connection stiffness and strength predicted by the BoF model were moreover compared to laboratory tests and the European Yield Model (EYM), which supported the validity of the BoF model. In addition, it was shown that the BoF model could enhance the prediction of the slip modulus compared to the current design regulations in Eurocode 5.

KEYWORDS: Beam-on-Foundation Model, CLT-to-concrete composite connections, connection stiffness

1 INTRODUCTION

The need for energy efficiency in construction has propelled the popularity of timber structures. Apart from exceptionally high mechanical properties in relation to the low weight of the material, timber has low mechanical properties under certain loading conditions and timber structures are prone to vibrations due to the lightweight nature of the material. The use of timber in combination with other construction materials in hybrid structures or structural composite elements, such as Timber Concrete Composites (TCC), can considerably improve the mechanical performance and stability as compared to conventional timber structures [1]. In TCC elements, timber and concrete elements are placed strategically in the tension and compression zones, respectively. Some of the benefits associated with TCC structures compared to timber structures are increased stiffness and load bearing capacity, improved sound insulation, reduced sensitivity to vibrations and improved structural bracing. In order to make use of the composite action in structural elements, efficient shear connections between the tension and compression-resisting components, i.e., between timber and concrete elements, are critical for the realization of the aforementioned benefits [2].

Most of the comprehensive experimental and numerical analyses of timber-concrete composite structures have been carried out with structural timber or glued laminated timber employed as the tension element. In recent years, studies on Cross Laminated Timber (CLT)-concrete composite structures have become increasingly popular. CLT is a pre-engineered timber product with an orthogonal laminar structure composed of an odd number of layers, usually with a maximum of seven layers. The popularity of CLT-to-concrete composite structures is attributed to improved mechanical properties in both longitudinal and transverse directions of CLT. CLT is attractive in development of full-scale wall and floor elements. CLT–concrete hybrid floor systems improve the bending capacity of the pure CLT floor elements by 3-5 times [3]. The suitability of common types of connectors such as, dowel-type fasteners [4], adhesive connections [5] and even novel types of connections [6] for CLT-to-concrete connections have been investigated by various researchers. Though adhesive connections provide an effective way to ensure a rigid shear connection between the concrete and CLT, shrinkage induced deflections of the composite connection render dowel-type connectors more suitable [1]. The stiffness of dowel-type connections in TCC elements depends on the deformation that takes place at the joint. Therefore, design of TCC connections assumes partial composite action, due to the difficulty in achieving full rigidity due to deformation at joints [7]. Ductility of dowel-type steel fasteners used in TCC connections increases the load-bearing capacity as well as the ultimate deformation capacity, because typically the connection shear capacity activates before the member ultimate load is reached [8]. However, ductile behaviour of the connection may not necessarily lead to ductile behaviour of the composite element if the stiffness of the

[1] Joan W. Gikonyo, Linnaeus University, Sweden, joan.gikonyo@lnu.se
[2] Eva Binder, Linnaeus University, Sweden, eva.binder@lnu.se
[3] Michael Schweigler, Linnaeus University, Sweden, michael.schweigler@lnu.se
[4] Thomas K. Bader, Linnaeus University, Sweden, thomas.bader@lnu.se

https://doi.org/10.52202/069179-0404

connection is higher than predicted, as the timber may exhibit brittle failure [2]. This emphasizes the importance of accurately predicting the slip modulus of TCC connections. Dias et al. [9] carried out a comparison between experimental tests on the load-bearing capacity of timber-to-concrete composite connections and the European Yield Model (EYM) by Ehlbeck and Larsen [10] in Eurocode 5 [11] (EC5) for i) timber-to-timber, ii) steel-to-timber and iii) timber-to-timber with a gap. The experimental results showed good agreement with all three EYM models. However, the EYM for steel-to-timber connections showed the best fit with the experimental results. Moreover, Dias et al. [12] compared experimental results for the slip modulus to i) analytical models based on beam-on-elastic foundation, and ii) the Eurocode-based empirical design equation for timber-to-timber connections, multiplied by a factor of two, as suggested in the code. The results showed that both models overestimated the slip modulus obtained in the experiments. Nonetheless, the experimental results showed better agreement with the Eurocode design equation.

The strength and slip modulus of TCC connections is experimentally determined according to EN 26891 [13]. However, Dias [14] showed that the connection slip modulus determined as per EN 26891 was inaccurate due to the pronounced non-linear response of TCC connections. Dias notes that the maximum slip observed in TCC connections is usually less than 8 mm, thus significantly lower than 15 mm indicated in EN 26891 [13], thereby, overestimating the shear capacity. Furthermore, it turns out that factors such as, initial slip [15], dowel diameter [6], concrete stiffness and strength [16] and connector inclination [4], influence the strength and slip modulus of CLT-to-concrete connections. The extent to which such factors influence the global response of CLT-to-concrete connection is largely unknown, which emphasizes the need for suitable design models for the prediction of both slip modulus and load bearing capacity of CLT-to-concrete connections.

The aim of this study is to validate a Beam-on-Foundation (BoF) model of CLT-to-concrete connections, by means of comparing model predictions with experimental results. The model is then applied to investigate the influence of various factors on the shear capacity and slip modulus of CLT-to-concrete connections. The outcome of this study provides experimental and numerical results that can be useful for creating structural design codes for CLT-concrete composite structures.

2 MATERIALS AND METHODS

2.1 Materials

The cross-laminated timber (CLT) elements, produced with boards of strength class C24 according to EN 338 [17], were stored in a climate room under standard climate conditions of 20°C and 65% RH for more than a year and it was assumed that an equilibrium moisture content of approximately 12% was established. The corresponding mean density of the CLT elements was 493 kg/m^3 (CV= 22%, 3 specimens). The prefabricated concrete elements were stored for at least 28 days before the tests, which leads to a stiffness of at least 33 GPa, with a mean density of 2371 kg/m^3 (CV= 1%, 3 specimens). The threaded rods for the connection had an ISO metric thread M24 and a quality of at least 8.8 grade steel.

2.2 Experimental tests on CLT-to-concrete shear connections

CLT-to-concrete connections were tested in a double shear push-out test configuration, see Figures 1 and 2. The tests were performed in a test frame, mounted with a hydraulic piston with a load capacity of up to 500 kN (MTS 210.45 G2, Flex test 60, MTS System Corporation, Sweden). In the test setup, the concrete element in the middle was connected by a threaded rod to two CLT side elements, kept together by a washer (d_{out}= 44 mm and d_{in}= 25 mm) and nut at each end, see Figure 1. The threaded rod was inserted into pre-drilled holes (d= 25 mm) in the timber and a casted hole in the concrete (d= 25 mm). A displacement-controlled load was applied to the concrete at a rate of 3 mm/min. Through a hinge included in the steel loading device, pure vertical loading and an even load distribution was ensured. The loading was stopped when the machine displacement reached 30 mm. The local displacement between concrete and CLT was measured with four linear variable differential transformers (LVDTs) – two on each side of the specimen. The mean local displacement of the LVDT measurements between the concrete and timber, the displacement, and the applied force from the testing machine over time were further processed and considered for the validation of the numerical model.

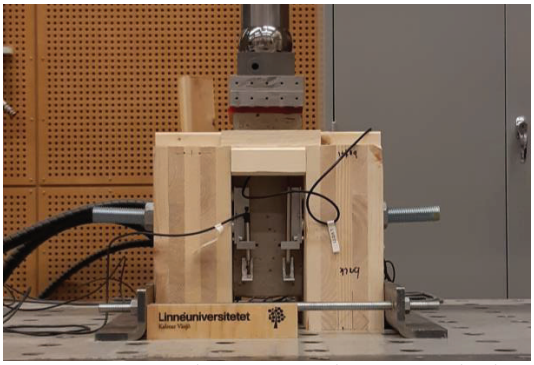

Figure 1: *Experimental test set-up used to carry out the shear test for the CLT-to-concrete connection.*

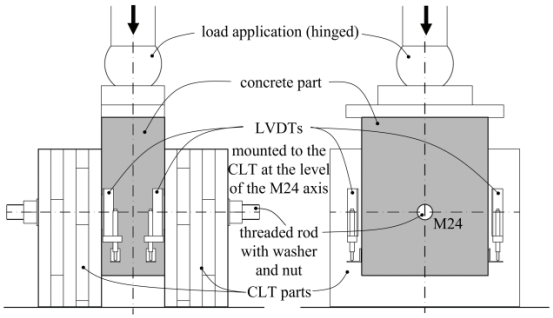

Figure 2: *Illustration of the experimental push-out test set-up for the CLT-to-concrete connection.*

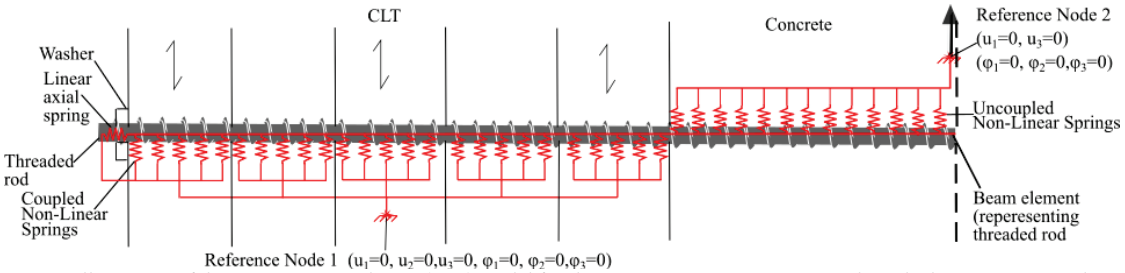

Figure 3: *Illustration of the Beam-on-Foundation (BoF) model for the CLT-to-concrete connection described in Section 2.2. The BoF model was created by considering symmetry and applying appropriate boundary conditions along the symmetry line.*

2.3 Numerical modelling of CLT-to-concrete connection using the BoF model

The 2-dimensional beam-on-foundation (BoF) model, illustrated in Figure 3, was used to simulate the CLT-to-concrete shear connection in the research presented herein. The model has been utilized by various researchers such as, Lemaitre et al. [18] and Schweigler et al. [19] to predict steel-to-timber connection behaviour, while considering non-linear embedment and elasto-plastic steel material behaviour. The model is composed of a deformable beam element that represents the steel fastener and rigid beams that host non-linear springs. These springs describe the local interaction between the steel fastener and the surrounding timber and concrete materials.

The model has four main inputs, a) the geometry of the connection, b) the non-linear load-slip data used to define the interaction between the steel dowel and, the i) concrete and ii) timber, c) the local interaction between washer and timber, and d) the mechanical properties of the steel fastener. Boundary conditions as regards the specimen support and the loading of the connection, as well as a possible lateral support at the washer or for symmetry conditions are specified at the reference nodes of the rigid elements and the fastener, see Figure 3.

2.3.1 Lateral embedment and axial withdrawal behaviour of timber

The non-linear load-slip data for the springs between the steel fastener and the CLT is defined using embedment load-slip data. The 2-dimensional BoF model considers two in-plane force components i) parallel to the fastener, related to the axial withdrawal capacity of the fastener and ii) perpendicular to the fastener, related to the lateral embedment behaviour of the fastener. The BoF model utilizes embedment load-slip data for both loading directions with respect to the grain direction of the timber, parallel and perpendicular to the grain, in the corresponding layers of the CLT. In lieu of experimentally determined embedment data for the connection materials, the analytical formula from Richard and Abbott [20] was used to determine the embedment stress, σ_h, in [MPa] at a particular displacement, u, in [mm] as,

$$\sigma_h(u) = \frac{(k_{f,el} - k_{f,pl}) \cdot u}{\left[1 + \left[\frac{(k_{f,el} - k_{f,pl}) \cdot u}{f_{h,inter}}\right]^a\right]^{\frac{1}{a}}} + k_{f,pl} \cdot u, \quad (1)$$

with the embedment parameters $k_{f,el}$ as the elastic foundation modulus in [N mm^{-3}] , $k_{f,pl}$ as the plastic foundation modulus in [N mm^{-3}], $f_{h,inter}$ as the intersection of the line defined by $k_{f,pl}$ with the y-axis in [MPa], and a as a transition parameter between $k_{f,el}$ and $k_{f,pl}$. The embedment parameters were determined using analytical formulas from a database [21] that includes several timber products, i.e., structural timber, Laminated Veneer Lumber (LVL), plywood and glulam, loaded both parallel and perpendicular to the grain as

$$f_{h,inter,0} = 0.1253 \cdot \rho - 20.32, \quad (2a)$$
$$f_{h,inter,90} = 0.1108 \cdot \rho - 28.47, \quad (2b)$$
$$k_{f,el,0} = 0.1374 \cdot \rho - 12.90, \quad (2c)$$
$$k_{f,el,90} = 0.0922 \cdot \rho - 18.20, \quad (2d)$$
$$k_{f,pl,0} = 0.0047 \cdot \rho - 2.0, \quad (2e)$$
$$k_{f,pl,90} = 0.0084 \cdot \rho - 2.21, \quad (2f)$$

where, ρ is the density of the timber in [kg m^{-3}]. In this study, the mean density of the CLT of 493 kg m^{-3} (see Section 2.1) was used to determine embedment parameters. It should be noted that the embedment parameter, $f_{h,inter,}$ in Equations (2a-b) was determined using the proposed formula for $f_{h,5mm}$ in [21]. Assuming the same dependence of the two parameters ($f_{h,inter,0}$ and $f_{h,inter,90}$) on the density, as for $f_{h,5mm,0}$ and $f_{h,5mm,90}$, might lead to a slight overestimation of the behaviour perpendicular to the grain. Figure 4 illustrates the embedment stress-displacement curves generated from Equations (2a-b) with consideration of the large displacement effect according to Schweigler et al. [19] when coupling the springs parallel and perpendicular to the fastener's axis. Only the component parallel to the loading direction of the connection, for loading parallel and perpendicular to the grain is shown in Figure 4. The non-linear stress-displacement data describing the axial capacity in between the fastener and the wood, was determined according to Schweigler et al. [19] with consideration of a friction coefficient, $\mu = 0.3$.

Once the stress displacement curves for both the embedment and axial (withdrawal) behaviour were determined, the corresponding forces of one embedment element in the model, $F(u)$, at a particular displacement, u, was calculated as,

$$F(u) = \sigma_h(u) \cdot d_{major} \cdot \Delta t \quad (3)$$

with the embedment stress, $\sigma_h(u)$ at that particular displacement, the major diameter of the threaded rod,

https://doi.org/10.52202/069179-0404

d_{major}, and the distance between adjacent springs, Δt. A single linear spring, positioned at the end of the fastener, simulated the axial resistance due to the washer. The stiffness of the axial spring of 3.9 kN/mm was determined, by considering the area of the washer of 994 mm^2 and the characteristic compression strength of the wood, $f_{c,90k}$, of 2.9 MPa, assuming a yield displacement of slightly less than 1 mm. The compressive strength was chosen equivalent to that of timber with an average density of 490 kg m^{-3} as per EN 338 [17], matching the mean density of the CLT. In dowel-type shear connections, and especially for fasteners inserted into pre-casted and pre-drilled holes, a clearance between the fastener and the surrounding material can be observed, which typically leads to an initial slip in the connection's load-displacement behaviour. Moreover, the indentation of the threaded part of the rod into the pre-drilled hole, leads to an initially softer behaviour, before full contact with the surrounding material is established. To consider this, the embedment stress-displacement curve is offset by a certain displacement representing the initial slip. The stiffness of the embedment curve up to the initial slip displacement was assumed to be 1% of the elastic foundation modulus, $k_{f,el}$.

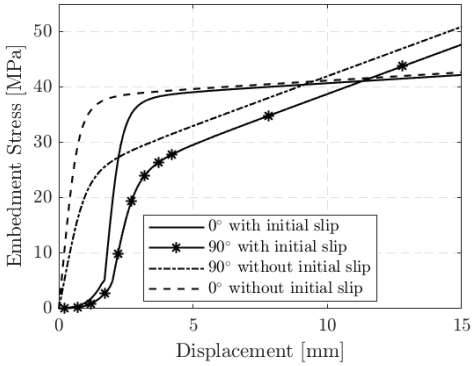

Figure 4: *Embedment stress-displacement curves of timber derived from embedment parameters using Equations (1) and (2).*

2.3.2 Concrete behaviour

The non-linear load-slip data for the interaction between the steel fastener and the concrete was determined as a multiple of the embedment parameters for the parallel loaded layer in the CLT. The values for $f_{h,inter}$ and $k_{f,el}$ were increased threefold, to account for the higher stiffness and compression strength of concrete, while for $k_{f,pl}$ the same values as for timber were used. Additionally, unlike the connectors between the steel fastener and the timber that were coupled, the connector elements parallel and perpendicular to the fastener's axis were uncoupled, since only small displacements were expected in the concrete, and thus, large displacement effects were neglected. In addition, connectors were only specified for the force resistance perpendicular to the fastener's axis, neglecting any possible axial resistance. Equations (1) and (2) were used to determine the stress-displacement curve for these non-linear spring connector elements. Subsequently, Equation (3) was used to determine the corresponding force-displacement data applied in the model.

2.3.3 Steel fastener

For the yield strength, the nominal values for steel quality 8.8 were increased by about 25%, since frequently higher yield and ultimate strength as compared to declared values were observed in connection tests. The remaining material properties of the threaded rod used in the BoF models presented herein were based on the properties of a dowel applied in [22]. Figure 5 shows the stress-strain relationship used in the model. Based on this stress-strain data, moment-rotation (bending angle) curves for various threaded steel rod diameters were determined using a numerical model of a 3-point bending test setup. In this study, consideration was made for both the major and minor diameter. The major diameter includes the depth of the thread while the minor diameter excludes the depth of the thread and thus is the diameter of the shank of the rod. The yield moment, $M_{y,R}$, was determined for a specific bending angle according to EN 409 [23] and further used in the analytical formulas provided in Eurocode 5 to determine the shear capacity of the CLT-to-concrete connections. In cases where the BoF model simulates threaded fasteners, the diameter of the threaded rod in the bending behaviour is specified as the minor diameter.

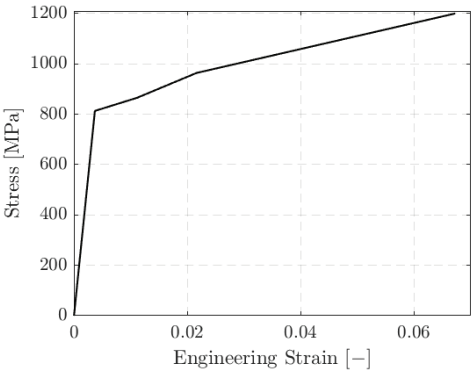

Figure 5: *Elasto-plastic response of the threaded steel rod.*

2.3.4 Evaluation of connection behaviour

After displacement-controlled loading at the reference node 2 in, shown in Figure 3**,** and the calculation of corresponding reaction forces at the support, the output from the BoF model is a force-displacement curve. The shear capacity and the slip modulus were determined according to EN 26891 [13]. Therefore, the shear capacity was defined as the maximum force up until 15 mm displacement. The slip modulus was determined as the gradient between the points at 10% and 40% of the shear capacity.

The results from the BoF model were compared to predictions of the European Yield Model (EYM) given by analytical formulas for the design of timber shear connections in Eurocode 5 (EC5) [11], for connections with a thick steel plate in steel-to-timber connections loaded in shear. This assumes a clamping of the fastener in the concrete (like in the steel) as compared to the considerably weaker behaviour of timber. EC5 determines the shear capacity, $F_{v,R}$, per shear plane for the

three failure modes associated with a thick steel plate for laterally loaded steel-to-timber connections as,

$$F_{v,R,mode1} = f_h t d_{major}, \quad (4a)$$

$$F_{v,R,mode2} = f_h t d_{major}\left(\sqrt{2+\frac{4M_{y,R}}{f_h t^2 d_{major}}}-1\right)+\frac{F_{ax,R}}{4}, \quad (4b)$$

$$F_{v,R,mode3} = 2.3\sqrt{2M_{y,R}f_h d_{major}}+\frac{F_{ax,R}}{4}, \quad (4c)$$

where, f_h is the embedment strength of timber or CLT in [MPa], $M_{y,R}$ is the yield moment of the fastener in [N mm], t is the thickness of the timber or CLT, d is the major diameter of the threaded rod in [mm] and $F_{ax,R}$ is the withdrawal capacity of the fastener. The contribution due to the rope effect, $F_{ax,R}/4$, representing the friction in the shear planes, was neglected as the friction in the shear plane was prevented in the experiments and BoF model. The yield moment, $M_{y,R}$, was determined at a particular angle of rotation, α, in [°] defined in EN 409 as,

$$\alpha = \alpha_1\left(\frac{2.78\cdot\rho}{f_t}\right)^{0.44}+\alpha_2, \quad (5)$$

where α_1 is the rotation angle in [°] dependent on the diameter of the dowel-type fastener, ρ is the density of the timber where the fastener is applied in [kg m^{-3}], f_t, is the tensile strength of the fastener in [MPa] and α_1 is 0° for dowels and bolts. In the standards, Equations (4) and (5) are based on characteristic values in a semi-probabilistic design concept. However, in this study mean values were applied to allow for a comparison with the experimental data and the BoF model predictions. The connection's serviceability slip modulus per shear plane, K_{ser} was determined as proposed in EC5 as,

$$K_{ser} = \frac{\rho_m^{1.5} d_{major}}{23} \quad (6)$$

where d_{major} is the major diameter of the threaded rod in [mm] and ρ_m is the mean density of wood in [kg m^{-3}]. EC5 proposes that for concrete (steel)-to-timber connections K_{ser} be multiplied by two as Equation (6) was derived for timber-to-timber connections.

3 RESULTS AND DISCUSSION

3.1 Model Validation

To validate the BoF model described in Section 2.3 it was used to predict the shear capacity and slip modulus of the experimentally investigated CLT-to-concrete shear connection detailed in Section 2.2. Symmetry and appropriate boundary conditions were used to create the BoF model, illustrated in Figure 3. A comparison of the shear capacity and slip modulus of the connection to i) the EYM and ii) the BoF model, was carried out. Figure 6 summarizes the results from the comparison also indicating the deformed shape of the fastener from the BoF simulations. The global force-displacement behaviour of the connection as predicted by the BoF model showed good agreement with the experimental results. Both the experiments and the BoF model illustrated ductile failure with substantial hardening past the yield point. Figure 6 shows the results from the BoF model, EYM and experiments. The slip modulus and shear capacity from the experiments and the BoF model were determined according to EN 26891 [13], as detailed in Section 2.3.4.

Meanwhile, for comparison to the EYM the embedment strength of CLT, f_h, was determined as the average embedment stress of the parallel and perpendicularly loaded layers (with initial slip from Figure 4) at 15 mm displacement, 44.8 MPa. The major diameter of the steel rod, 24 mm, was used to calculate the embedment force-displacement data of wood. Similarly, when determining the shear capacity according to the EYM, the major diameter was used. However, the minor diameter of the steel rod, 20.3 mm, was assumed to determine the moment resistance of the threaded steel rod, which yielded a plastic moment of $M_{y,R} = 1169$ kN mm. The contribution from the rope effect was neglected as the test set-up ensured no friction occurred between the concrete and CLT surfaces.

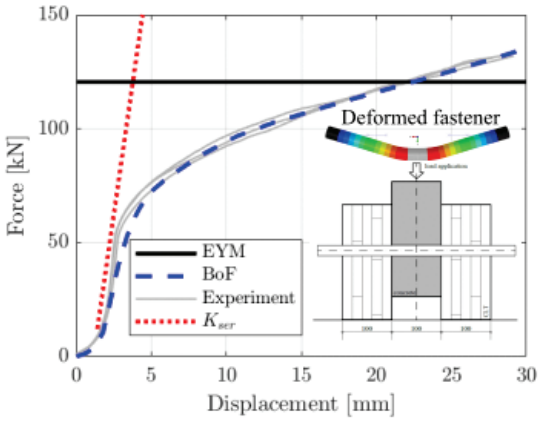

Figure 6: *Comparison of the global force-displacement results from the experiments to the BoF prediction and the EYM according to Eurocode 5.*

The results, summarised in Table 1, revealed that the EYM overestimated the shear capacity of the connection by 13%. On the contrary, the BoF model predicted the shear capacity rather accurately. The EYM assumes full utilization of the plastic moment of the fastener and ideal plastic behaviour of the wood embedment, which in the experiments and BoF model is not reached for all areas along the fastener. The BoF model underestimated the slip modulus by 20%. On the contrary, K_{ser} overestimated the slip modulus by 29%. The overestimation of K_{ser} is similar to what Dias et al. observed in [14]. The underestimation from the BoF model was attributed to the use of the minor diameter instead of the major or effective diameter of the threaded steel rod which results in a lower embedment stiffness and lower yield moment, $M_{y,R}$, of the threaded steel rod, and thus, lower shear capacity and slip modulus. The deformed shapes of the fastener from the BoF model and experiment agreed well with failure mode 2 from EYM, characterized by clamping of the fastener in the concrete with a deformation of the fastener in the CLT.

https://doi.org/10.52202/069179-0404

Table 1: *Comparison of BoF model and the EYM predictions to the experimental results of the CLT-to-concrete connection.*

Shear capacity [kN]			Slip Modulus [kNmm^{-1}]		
EYM	BoF	Experiment	K_{ser}	BoF	Experiment
120.6	106.5	107.2	45.7	28.4	35.5

3.2 Parameter study

A preliminary parameter study was carried out to investigate the influence of dowel diameter, initial slip, concrete stiffness, friction along the fastener, and axial resistance due to the washer on the global force-displacement response of the BoF model prediction discussed in Section 3.1. In this parameter study, only one parameter alteration was done per study, as compared to the reference connection. The results, shown in Figure 7, indicate that altering any of these five parameters resulted in a change in the global force-displacement response of the connection, thereby influencing the connection shear capacity and slip modulus.

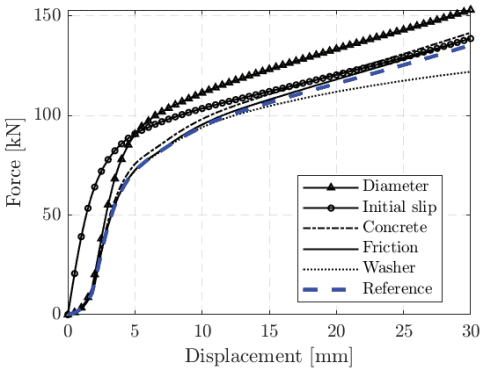

Figure 7: *Initial parameter study of various factors that influence the force-displacement behaviour of the CLT-to-concrete reference shear connections.*

The results from this preliminary parameter study are summarised in Table 2. The slip modulus and shear capacity of the connection were assessed according to EN 26891 [13]. This investigation revealed that assuming the major instead of the minor diameter of the rod yielded the highest increase in shear capacity of the reference connection by up to 16%. Additionally, neglecting initial slip, assuming stiffer and stronger concrete and a higher friction coefficient resulted in 5%, 4% and 1% increase in shear capacity, respectively. However, neglecting the washer yielded a reduction of the shear capacity by 2%. Moreover, the study of the aforementioned parameters shows that, neglecting the initial slip resulted in the highest increase in the slip modulus of 28%. Furthermore, assuming the major instead of the minor diameter, stiffer and stronger concrete and a higher coefficient of friction caused 18%, 6% and 1% increase in the slip modulus, respectively. Neglecting the washer had negligible influence on the slip modulus. However, upon further assessment it was evident that the influence of the washer and friction were more important for the behaviour beyond 15 mm displacement. Furthermore, the effect of the washer is overlaid with the effect of the friction along the fastener between fastener and CLT. A 1% increase in the force due to an increased friction coefficient was found at 9 mm displacement. The force further increased with increased fastener displacement, finally yielding 3% higher force than the reference connection at 30 mm displacement. Similarly, the influence of the withdrawal capacity due to the washer was observable beyond a displacement of 13 mm, where the force was 1% lower than in the reference connection. Increased displacement showed a marked increase of the influence of the washer. At a maximum displacement of 30 mm, neglecting the washer yielded a 10% lower force.

Table 2. *Influence of various parameters on the shear capacity and slip modulus of the reference connection.*

Parameter	Reference Value	New value	Shear capacity	Slip modulus
Diameter	20.3 mm	24 mm	+16%	+18%
Initial slip	2 mm	0 mm	+5%	+28%
Concrete	$3 \cdot f_{h,inter}$ $3 \cdot k_{f,el}$	$4 \cdot f_{h,inter}$ $4 \cdot k_{f,el}$	+4%	+6%
Friction	0.3	0.4	+1%	+1%
Washer	Included	Neglected	-2%	~0%

With these findings, an in-depth parameter study was done to look further into the influence of four out of the five aforementioned parameters. The influence of the washer capacity on the connection shear capacity is not presented since a similar behaviour as for the coefficient of friction was seen. As a reference, the connection illustrated in Figure 3 was used. Three important items should be noted to guide the discussion hereafter regarding the reference connection: i) embedment stress-displacement data was used without the initial slip, see Figure 4, ii) the washer was neglected, and iii) the threaded rod was modelled using the major diameter. All other properties of the BoF model, the elasto-plastic behaviour of the threaded rod and concrete embedment properties were used as specified in Section 2.

3.2.1 Diameter of threaded rod

The diameter of a fastener influences its mechanical properties as the moment resistance increases with increase in the diameter. Therefore, it follows that using the major diameter of the threaded rod will result in increased shear capacity and slip modulus. However, assuming the major diameter, d_{major}, implies that the shank of the threaded rod is larger. To investigate the influence of assuming the yield moment for the minor or major diameter, i.e., d_{minor} or d_{major} for modelling the threaded steel rod, several BoF models were created for various threaded steel rods major diameters, 10 mm $\leq d_{major} \leq$ 30 mm. The ratio of d_{minor} to d_{major} ranged between 0.88 and 0.83. For the BoF simulations, firstly, the threaded steel rod was modelled using d_{major}, like in the reference model, and secondly, variant models of the reference connection were created with the threaded steel rod modelled using the d_{minor}. For both models, the force-displacement data used for the wood in the CLT, determined according to Equation (5), was calculated using the d_{major}. Furthermore, the results were compared to the EYM. In the latter, the rope effect, representing the friction in the shear planes, was neglected as the friction

https://doi.org/10.52202/069179-0404

in the shear plane was prevented in the experiments and BoF model. The yield moment applied in the EYM was determined for the maximum bending angle, α, using i) d_{minor} and ii) d_{major} according to EN 409 [23].

The results showed that assuming the yield moment from d_{minor} resulted in reduced shear capacity and slip modulus for both the BoF model and the EYM, see Figure 8. This was attributed to the reduced mechanical properties of the fastener. A comparison between the BoF model predictions showed that assuming d_{minor} resulted in up to 21% reduction in shear capacity for the 10 mm threaded rod. The reduction in shear capacity was lower for larger diameters of the threaded rod. The BoF model for the 30 mm threaded rod showed 14% reduction in shear capacity.

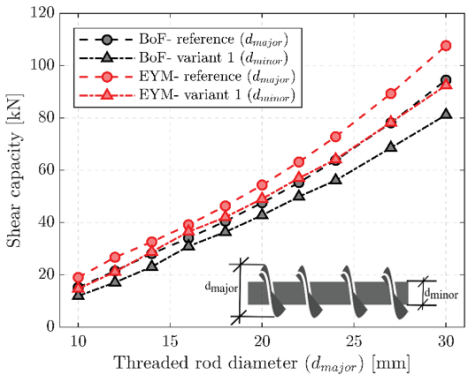

Figure 8: *Comparison of the BoF model and EYM predictions for shear capacity of a CLT-to-concrete connection, per shear plane, while using the minor and major diameter.*

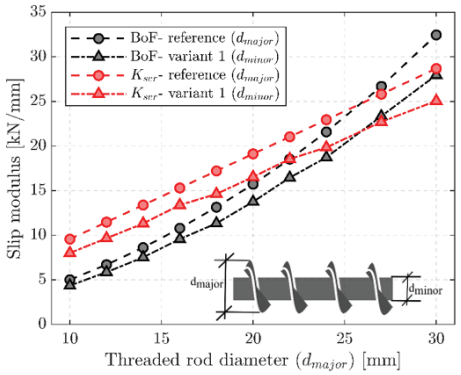

Figure 9: *Comparison of the BoF model and K_{ser} predictions for slip modulus of a CLT-to-concrete connection, per shear plane, while using the minor and major diameter.*

A comparison of the results from the BoF models to the EYM showed that shear capacity predicted from the EYM was on average 15% and 17% higher than the equivalent BoF model predictions utilizing the d_{major} and d_{minor}, respectively. The difference was highest at smaller diameters of the threaded rod with up to 20% and 19% higher shear capacity in the EYM than the BoF model with d_{major} and d_{minor}, respectively. The difference between EYM and BoF model could be because the EYM assumes full utilization of the plastic moment of the fastener and ideal plastic behaviour of the wood embedment, which in the BoF model is not reached for all areas along the fastener. Thus, the EYM will give an upper limit for the connection capacity if the input for the embedment strength is used as assumed in this study. An analysis of the connection's slip modulus showed that BoF models that utilized d_{major} yielded on average 13% higher slip modulus compared to equivalent BoF models that utilized d_{minor}, see Figure 9. The comparison between K_{ser} and BoF model predictions for connection slip modulus showed that K_{ser} yielded higher slip modulus. The difference was highest for small dowel diameters with up to 48% and 56% higher K_{ser} as compared to equivalent BoF models that utilized d_{major} and d_{minor}, respectively. The difference reduced with increased dowel diameter, with models utilizing threaded rod major diameters, d_{major}, ranging between, 24 mm < d_{major} < 26 mm, showing rather good agreement with K_{ser}. However, for threaded rods with diameters, d_{major} > 26 mm, K_{ser} yielded a lower slip modulus of the CLT-to-concrete connection as compared to the BoF model. These findings highlight the disadvantage of K_{ser} being defined independent of the connection failure mode, resulting in a substantial simplification for certain connection layouts.

3.2.2 Initial slip

Initial slip refers to the displacement that occurs between fastener and borehole before full contact is achieved with the surrounding timber matrix. This phenomenon leads to a reduced initial elastic foundation modulus, $k_{f,el}$, for the wood as detailed in Section 2.3.1. Therefore, this parameter study investigates the influence of the initial slip on the shear capacity and slip modulus of CLT-to-concrete connections. Several models of the CLT-to-concrete connection were created for various threaded rod diameters from 10 mm to 30 mm, using the BoF model with embedment stress-displacement data i), without initial slip (reference) and ii) with initial slip (Variant 1), illustrated in Figure 4. The results showed that BoF models of the reference CLT-to-concrete connection with initial slip yielded on average 4% lower shear capacity in comparison to equivalent BoF models without initial slip, see Figure 10. A similar difference was found for the EYM predictions. This was attributed to the reduced embedment strength for the models with the initial slip. Accounting for the initial slip leads to a shift of the embedment curve. Thus, same absolute displacement values give lower embedment stress for the models with initial slip, especially for embedment loading perpendicular to the grain, which shows an increase in embedment stress after yielding. This effect is reflected also in the embedment strength definition, where f_h was determined at 15 mm displacement according to EN 26891 [13]. The comparison of the BoF model with the EYM showed that the EYM yielded a higher connection shear capacity for both models, i.e. variant 1 and reference, on average 16% and 15%, respectively. The EYMs with smaller threaded rod diameters when compared to their equivalent BoF models showed up to 20% higher shear capacity. Similar to the previous study on the diameter of the threaded rod, the difference reduced with increased diameter. The effect of the initial slip on the connection slip modulus was similar to that on the shear capacity, as the initial slip resulted in a reduced slip

https://doi.org/10.52202/069179-0404

modulus, see Figure 11. In addition to an initial weaker overall response of the connection, the lower slip modulus is also given due to reduced shear capacity that determined the points at 10% and 40% of the shear capacity, between which the slip modulus was determined. The lower point at 10% of the shear capacity was found to be located in the initial softer part of the load-displacement curve, which resulted in a reduced slip modulus of the connection. Consideration of the initial slip caused on average 28% reduction in slip modulus. Moreover, an analysis of variant 1 BoF models, that considered initial slip, showed that K_{ser} prediction yielded a higher slip modulus of all variant 1 BoF models of the CLT-to-concrete connection for various threaded rod diameters. The results for the comparison of the reference BoF models and their equivalent EYMs is as detailed in Section 3.2.1.

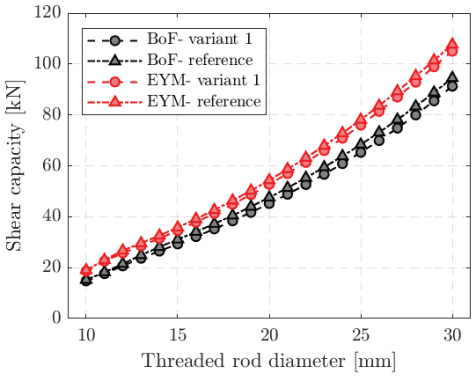

Figure 10: *Comparison of the BoF model and EYM predictions for shear capacity of a CLT-to-concrete connection, per shear plane, to investigate the influence of initial load slip.*

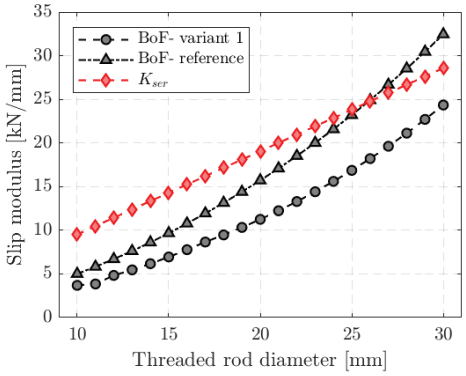

Figure 11: *Comparison of the BoF model and K_{ser} predictions for slip modulus of a CLT-to-concrete connection, per shear plane, to investigate the influence of initial load slip.*

3.2.3 Embedment stiffness and strength of concrete

The stiffness and strength parameters used to determine the load-displacement data for the interaction between the threaded steel rod and the concrete, detailed in Section 2.3.2, were based on the wood properties parallel to the grain and multiplied by a factor of 2 (BoF model variant 1), factor of 3 (reference BoF model) and factor of 4 (BoF model variant 2). The results from this study showed that there was on average 3% increase in shear capacity of the reference connection when the strength and stiffness of the concrete was increased, see Figure 12. Conversely, the shear capacity decreased on average by 6%, with decrease in the concrete strength and stiffness. This difference in the shear capacity due to altering the concrete strength and stiffness was most pronounced for BoF models with diameters less than 13 mm. A comparison of the BoF models with the EYM showed that the EYM yielded a higher shear capacity of 19%, 15% and 12%, than for variant 1, reference connection and variant 2 BoF models, respectively.

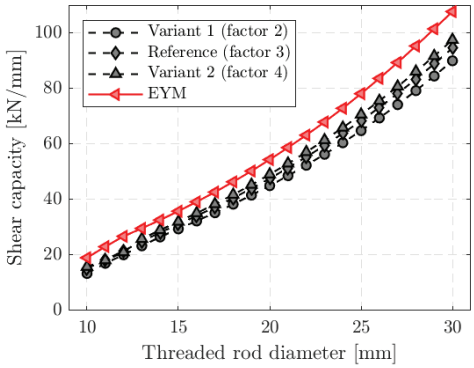

Figure 12: *Comparison of the BoF model and EYM predictions for shear capacity of a CLT-to-concrete connection, per shear plane, to investigate the influence of concrete stiffness and strength.*

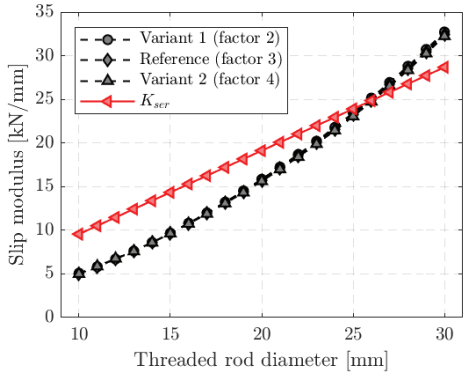

Figure 13: *Comparison of the BoF model and K_{ser} predictions for slip modulus of a CLT-to-concrete connection, per shear plane, to investigate the influence of concrete stiffness and strength.*

The reduction in the difference in the shear capacity between the EYM and the BoF models with increase in concrete strength and stiffness was attributed to increased bending deformation of the fastener within the CLT due to increased clamping. The EYM highlights that the shear capacity is directly linked with the corresponding failure modes [11]. If the side member thickness, in this case concrete, is larger than that of the diameter, failure mode 2 characterized by development of a single plastic hinge in the side member is observed according to the EYM. Therefore, Equation 4(b) was used to determine the shear capacity of the connection. The yield moment associated with this connection was determined for a certain bending angle, α, according to EN 409 [23]. Increasing the concrete stiffness and strength increased the clamping of

the fastener within the concrete whilst increasing the rotation of the fastener in the CLT. Increased fastener rotation led to activation of more spring connector elements in the CLT, and in addition to a larger resistance per spring, due to the larger spring connector displacements, hence increasing the shear capacity. Contrary to the findings on shear capacity, increasing the strength and stiffness of concrete had negligible effect on the slip modulus of the connection, see Figure 13. A comparison of the results from BoF models, variant 1 and variant 2, to equivalent BoF models of the reference connection for varying diameters, showed less than 1% difference. Similar to previous studies, K_{ser} yielded higher slip modulus for most of the BoF models considered. The results were similar to the comparison of reference BoF model to equivalent EYM detailed in Section 3.2.1.

3.2.4 Friction

The influence of friction between the rod and the wood on the shear capacity and slip modulus of CLT-to-concrete connections was investigated for various diameters of the threaded rod. The friction coefficient, μ. was altered, such that for each threaded steel rod considered for this study, two variants of the reference BoF model (μ=0.3), were created. BoF model variant 1 assumed μ=0 and BoF model variant 2 assumed μ=0.6.

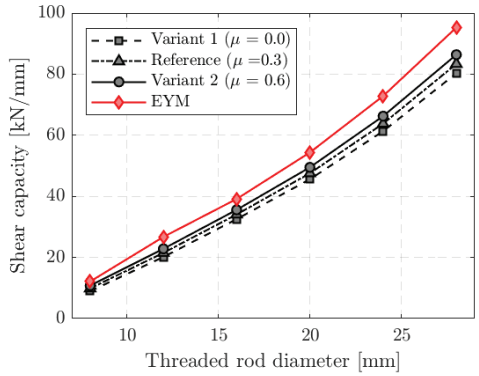

Figure 14: *Comparison of the BoF model and EYM predictions for shear capacity of a CLT-to-concrete connection, per shear plane, to investigate the influence of friction.*

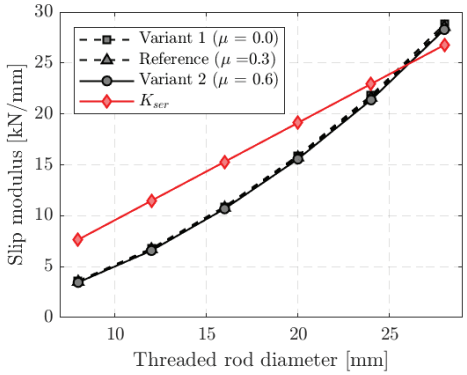

Figure 15: *Comparison of the BoF model and K_{ser} predictions for slip modulus of a CLT-to-concrete connection, per shear plane, to investigate the influence of friction.*

A comparison of the reference BoF model with variant 1 and 2 was carried out. The results showed that increasing the friction coefficient in BoF model variant 2 led to a subsequent increase in the shear capacity. On average, this increase was 5%, with higher relative increase for smaller threaded rod diameters, see Figure 14. Similarly, assuming no friction, i.e., μ=0 in BoF model variant 1 led to a 5% reduction in shear capacity when compared to the reference model. As discussed for the preliminary parameter study in Section 3.2, a considerable large connection displacement is needed to cause a substantial inclination of the fastener, to take an effect of the axial force component caused by friction on the connection shear resistance. The EYM prediction was not influenced by a change in the friction coefficient. On average, the EYM recorded, 18%, 13% and 9% higher shear capacity than BoF model variant 1, reference BoF model and BoF model variant 2, respectively. Similar to the findings in the parameter study on the influence of concrete stiffness and strength, in Section 3.2.3, there was negligible influence of the friction coefficient on the slip modulus of the connection, see Figure 15. These findings are similar to results from a parameter study on the influence of the axial fastener behaviour on the shear capacity of steel-to-timber connections in [19].

4 CONCLUSIONS

The beam-on-foundation (BoF) method was applied herein to predict the shear capacity and slip modulus of CLT-to-concrete connections. The parameter study rests on a validation of the BoF model with experiments on a CLT-to-concrete connection with a single threaded rod. Results indicated validity of the BoF model for this application by a good agreement of the nonlinear load-displacement behaviour, and thus of the shear capacity and slip modulus, between simulations and experiments. From the comprehensive parameter study, it can be concluded that:

- Shear capacity and slip modulus are substantially influenced by the choice of either using the minor or major diameter of the threaded rod for BoF simulations and EYM predictions.
- Consideration of the initial slip in the BoF model results in reduced shear capacity and slip modulus of CLT-to-concrete connections, determined according to EN 26891.
- Varying the friction coefficient between rod and wood between 0-0.6 and varying the embedment properties of concrete had negligible influence on the slip modulus, and only a minor influence on the shear capacity of the investigated CLT-to-concrete connections.
- K_{ser} proposed in EC5 was found to give simplified slip modulus predictions for CLT-to-concrete connections, since the influences of parameters like e.g. the fastener slenderness, are not considered in the design equation, but their impact was shown by the BoF model.

The BoF model was found to be useful in determining both the slip modulus and shear capacity of the connection. Application of the model in engineering

https://doi.org/10.52202/069179-0404

design can lead to more reliable and economic connections in CLT-to concrete composite slabs.

5 ACKNOWLEDGEMENT

The authors would like to acknowledge the support from the Knowledge Foundation through the project 'Improving the competitive advantage of CLT-based building systems through engineering design and reduced carbon footprint' (project number 20190026).

6 References

[1] A. Siddika, M. A. A. Mamun, F. Aslani and Y. Zhuge, "Cross-laminated timber–concrete composite structural floor system: A state-of-the-art review," *Engineering Failure Analysis,* vol. 130, 2021.

[2] A. Ceccotti, "Composite concrete-timber structures," *Progress in Structural Engineering and Materials,* vol. 4, no. 3, pp. 264-275, 2002.

[3] K. Quang Mai, A. Park, K. T. Nguyen and K. Lee, "Full-scale static and dynamic experiments of hybrid CLT–concrete composite floor," *Construction and Building Materials,* vol. 170, pp. 55-65, 2018.

[4] K. Mai, A. Park and K. Lee, "Experimental and numerical performance of shear connections in CLT–concrete composite floor," *Materials and Structures,* vol. 51, 2018.

[5] V. Bajzecerová, J. Kanócz, M. Rovňák and Maroš Kováč, "Prestressed CLT-concrete composite panels with adhesive shear connection," *Journal of Building Engineering,* vol. 56, 2022.

[6] A. Samuel C., S. Luca and S. Alexander, "A new composite connector for timber-concrete composite structures," *Construction and Building Materials,* vol. 112, pp. 84-92, 2016.

[7] Y. Jiang and R. Crocetti, "CLT-concrete composite floors with notched shear connectors," *Construction and Building Materials,* vol. 195, pp. 127-139, 2019.

[8] D. Alfredo M.P.G. and J. Luís F.C., "The effect of ductile connectors on the behaviour of timber–concrete composite beams," *Engineering Structures,* vol. 33, no. 11, pp. 3033-3042, 2011.

[9] A. M. P. G. Dias, S. M. R. Lopes, J. W. G. V. d. Kuilen and a. H. M. P. Cruz, "Load-Carrying Capacity of Timber–Concrete Joints with Dowel-Type Fasteners," *Journal of Structural Engineering,* vol. 133, no. 5, pp. 720-727, 2007.

[10] J. Ehlbeck and H. Larsen, "Eurocode 5 - Design of timber structures: Joints," in *International Workshop on Wood Connectors*, 1993.

[11] EN 1995-1-1, Design of timber structures—Part 1-1: General—Common rules and rules for builidngs., Brussels: (CEN), European Committee for Standardization, 2011.

[12] A. Dias, H. Cruz, S. Lopes and J. van de Kuilen, "Stiffness of dowel-type fasteners in timber-concrete joints," *Proceedings of the Institution of Civil Engineers - Structures and Buildings,* vol. 163, no. 4, pp. 257-266, 2010.

[13] EN 26 891: 1991 Timber structures - Joints made with mechanical fasteners - General principles for the determination of strength and deformation characteristics, Brussels: (CEN), European Committee for Standardization, 1991.

[14] A. M. P. G. Dias, Mechanical behaviour of timber-concrete joints, (doctoral thesis), Delft University of Technology, 2005.

[15] J. Cao, H. Xiong, Z. Wang, Chen and Jiawei, "Mechanical characteristics and analytical model of CLT-concrete composite connections under monotonic loading," *Construction and Building Materials,* vol. 335, 2022.

[16] J. Luis Filipe Carvalho, S. M. Rodrigues, Lopes and C. and Helena Maria Pires, "Interlayer Influence on Timber-LWAC Composite Structures with Screw Connections," *Journal of structural engineering,* vol. 137, no. 5, 2011.

[17] EN 338:2016 Structural timber – Strength classes, Brusssels: (CEN), European Committee for Standardization, 2016.

[18] R. Lemaitre, J. Bocquet, M. Schweigler and T. Bader, "Beam-on-foundation modelling as an alternative design method for timber joints with dowel-type fasteners: Part 1: Strength and stiffness per shear plane of single-fastener joints.," in *International Network on Timber Engineering Research (INTER) , Meeting 51*, Talllinn, Estonia, 2018.

[19] M. Schweigler, M. Vedovelli, R. Lemaître, J.-F. Bocquet, C. Sandhaas and T. K. Bader, "Beam-on-Foundation Modeling as an Alternative Design Method for Timber Joints with Dowel-Type Fasteners –Part 3: Second Order Theory Effects for Considering the Rope Effect," in *International Network on Timber Engineering Research*, 2021.

[20] R. M. Richard and B. J. Abbott, "Versatile Elastic-Plastic Stress-Strain Formula," *Journal of the Engineering Mechanics Division,* vol. 101, 1975.

[21] M. Schweigler, T. K. Bader, J.-F. Bocquet, R. Lemaître and C. Sandhaas, "Embedment test analysis and data in the context of phenomenological modeling for dowelled timber joint design," in *International Network on Timber Engineering Research*, Tacoma, WA, USA, 2019.

[22] ADIVbois, "Technical report – experimental characterization of connection stiffness (in French, not published yet)".

[23] EN 409 Timber Structures - Test methods - Deyermination of the yield moment of dowel type fasteners, Brussels: (CEN), European Committee for Standardization, 2009.